Influence of Shear on Lyotropic Lamellar Phases with Different Membrane Defects

Johannes Zipfel,[†,‡] Jörg Berghausen,[†] Peter Lindner,[‡] and Walter Richtering*[,†]

Albert-Ludwigs-Universität Freiburg, Institut für Makromolekulare Chemie, Stefan-Meier-Strasse 31, D-79104 Freiburg i. Br., Germany, and Institut Laue-Langevin, B.P. 156, F-38042 Grenoble, France

Received: September 30, 1998; In Final Form: January 26, 1999

The influence of shear on lyotropic lamellar phases in the system sodium dodecyl sulfate (SDS)/decanol/water has been studied using small angle neutron and light scattering (SANS, SALS), birefringence and rheology. Eight different samples with a constant water content of 67.4%, but different surfactant-cosurfactant ratio were studied. Static SANS measurements showed that replacing of SDS with decanol leads to a transition from a defective lamellar phase, characterized first by a ribbon like structure and then by a pore like structure, to a classical lamellar phase. An orientation diagram was obtained from SANS, SALS and birefringence measurements under shear. For samples with low decanol content, shear flow leads to an alignment of lamellae but in addition to previous studies, we found two reorientations, from a parallel (at low shear rates) to a perpendicular alignment of the lamellae (with respect to the walls of the shear cell) and to a parallel alignment again at the highest shear rates available. At intermediate decanol content, a shear induced formation of multilamellar vesicles was observed in a certain shear rate region. Samples with classical lamellar structure at high decanol content exhibited no shear induced vesicle formation.

1. Introduction

Shear flow is known to have a profound influence on the orientation and structure of complex fluids.[1−3] Especially lamellar systems have attracted attention in the past few years, and they are formed in such different materials as polymer melts and surfactant solutions. Shear orientation was reported for both kinds of materials and different states of orientation could be observed. Following the terminology used in other work[4] we denote the three possible real space orientations of lamellae according to the direction of the layer normal. Orientation of the layer normal along the vorticity direction, the flow direction and the velocity gradient direction are denoted as *a* ("perpendicular"), *b* ("transpose"), and *c* ("parallel"), respectively.

Studies with large amplitude oscillatory shear on block copolymer systems have revealed different orientations of the lamellae.[5−7] At low frequencies the lamellae are oriented with the layer normal parallel to the velocity gradient (*c*-orientation); at high frequencies, however, they are oriented with the layer normal parallel to the vorticity direction (*a*-orientation). It has been suggested that the stability of the perpendicular orientation is caused by layer fluctuations close to the order−disorder transition.[8,9] Recently a second transition from perpendicular to parallel orientation was found.[5]

Lyotropic lamellar phases also show different behavior under shear. While Roux and co-workers detected a parallel alignment of the lamellae,[10] a transition to the perpendicular orientation has been observed in other systems.[11−14] In contrast to block copolymer melts, solutions of low molar mass surfactants and of amphiphilic block copolymers also showed a formation of shear induced multilamellar vesicles MLVs (onions)[10,12,15−18] the size of which was correlated with either the shear rate[10] or the shear stress.[12] These vesicle phases could, depending on the shearing conditions, be either densely packed in a glasslike amorphous structure[10] or structured in a hexagonal packing.[19] Very recently a jump from a population of smaller vesicles to a population with bigger vesicles was detected by increasing the shear rate.[20] Hoffmann and co-workers studied shear effects during the preparation of diluted vesicular phases[21] and found a transition from multilamellar into small unilamellar vesicles at high shear rates.[22] Our group recently detected a transition to a state where the multilamellar vesicles are disordered in the direction of flow, which can be characterized by a butterfly type pattern at low scattering angles in small angle neutron scattering (SANS).[23] Obviously, the influence of shear flow on the orientation in lamellar systems can be manifold.

Less is known, however, about the influence of shear on intermediate phase systems near the lamellar phase, especially disk-shaped micelles or defective lamellar phases. Recent experiments have shown that the building blocks of the phases at the transition from nematic discotic to lamellar phases may differ from the classical picture of disk-shaped micelles and continuous lamellae. Studies on the binary system of cesium pentadecafluorooctanoate/water and the ternary system of sodium decyl sulfate/decanol/water revealed the formation of a defective lamellar phase ($L_\alpha H$) where the continuous lamellae were broken by elongated water filled holes.[24,25] Recent investigations on binary systems have also shown that the transition from nematic discotic to defective lamellar phases is almost imperceptible from static small angle X-ray and neutron scattering experiments.[26]

Mang and co-workers studied the effect of shear on nematic and lamellar phases in aqueous solutions of cesium perfluorooctanoate.[11] The L_α-phases oriented in the perpendicular orientation while the nematic phase was found to align with the director parallel to the velocity gradient (orientation *c*). They observed subtle shear-rate dependent director reorientations from *c* to *a* in the proximity of the N-to L_α-phase transition. Penfold

* To whom correspondence should be sent. e-mail: rich@uni-freiburg.de. Fax: +49 761 203-6319.
† Albert-Ludwigs-Universität Freiburg.
‡ Institut Laue-Langevin.

10.1021/jp983917h CCC: $18.00
Published on Web 03/30/1999

TABLE 1: Molar Decanol Fraction x_c, Volume Fraction ϕ_u of the Membrane and Composition in Weight Percent for All Samples as Well as the Lamellar Spacing $d_{||}$ and the Characteristic Distance between Defects $d_{\perp}$[a]

	sample							
	1	2	3	4	5	6	7	8
x_c	0.285	0.301	0.313	0.326	0.354	0.367	0.411	0.444
ϕ_u	0.289	0.293	0.293	0.297	0.300	0.301	0.304	0.303
SDS (w/w %)	26.77	26.40	26.10	25.78	25.09	24.75	23.60	22.69
decanol (w/w %)	5.86	6.23	6.53	6.86	7.55	7.88	9.04	9.94
D_2O (w/w %)	67.37	67.37	67.37	67.37	67.37	67.37	67.37	67.37
$d_{||}$ (Å)	58.5	59.4	60.8	62.0	65.9	67.1	76.2	78.4
$d_{\perp}$ (Å)	88.7	95.8	96.8	106.5	119.7	130.7		
$d_{||}^w$ (Å)	35.5	36.3	37.7	38.8	42.6	43.8	52.7	54.7
$d_{\perp}^w$ (Å) ribbons	18.7	19.2	17.3	17.0	13.2	12.6		
$d_{\perp}^w$ (Å) pores	−7.7	−3.5	0.7	6.6	21.8	31.0		
$d_{\perp}^w$ (Å) holes	−8.2	−9.5	−11.0	−13.4	−18.9	−21.6		

[a] In addition to this, the data calculated according to the model by Holmes et al.[25] for the different types of membrane defects (see Figure 3) are given.

and co-workers[13] also observed a reorientation from the parallel to the perpendicular orientation at high shear rates for a defective lamellar phase of hexaethylene glycol monohexadecyl ether. While phase transitions can be induced by temperature changes for binary systems, replacing a surfactant by a cosurfactant thus changing the mean curvature of the micellar aggregate can lead to similar transitions in ternary systems.

Hendrikx[27] and Quist[28] studied in detail these structural transitions in the system sodium decyl sulfate/decanol/water. Our investigations are based on a work by Berger and Hiltrop[29] on the system sodium dodecyl sulfate/decanol/water. They found that the interplanar distances from the hexagonal to the lamellar phases gradually changed without any discontinuity. We recently studied a defective lamellar phase of this system and detected a second reorientation from parallel to perpendicular at very high shear rates.[30] A similar *a*-to-*c* transition was recently also reported from a different system.[31] At a higher decanol content we observed only one reorientation which was shifted up to higher shear rates and the formation of multilamellar vesicles.[32]

The aim of this study was to investigate the influence of membrane defects on shear orientation. A previous study already proved the shear induced formation of MLVs in defective lamellar phases,[33] but a recent investigation of a different system suggested that membrane defect might hinder the MLV formation.[34] Therefore an orientation diagram for the system SDS/decanol/water had to be constructed which characterizes the various structures as a function of shear rate and surfactant/cosurfactant ratio. Eight samples with a constant water content of 67.4%, but different surfactant−cosurfactant ratios were studied. Some results from two samples have been reported before, but they are mentioned here again in order to discuss the influence of surfactant−cosurfactant ratio.

To elucidate structural transitions in this series, we investigated all samples with SANS at rest on a broad range of momentum transfer q. For measurements under shear, we used SANS, small angle light scattering (SALS), and birefringence. SANS is a suitable tool for the study of shear induced structural changes. Especially the so-called tangential position where the neutrons pass through the side of a Couette type shear cell proved to be a powerful means in order to distinguish between the different possible orientations of lamellar phases under shear. Flow birefringence can also indicate transitions between different orientations.

2. Experimental Details

Materials and Sample Preparation. 1-Decanol (99%) was purchased from Sigma-Aldrich, sodium dodecyl sulfate (>99%) from Fluka. All chemicals were used without further purification. The samples were prepared by weighing the appropriate amounts of SDS, decanol and heavy water into a glass tube. Then they were rigorously mixed for 2 days and allowed to equilibrate for at least 2 weeks. The defective lamellar phase consisted of sodium dodecyl sulfate/decanol/D_2O with a D_2O mass fraction of 0.674. Eight different samples with different molar fraction x_c of decanol in the surfactant/cosurfactant mixtures were investigated. All experiments were performed at 25 °C. Table 1 summarizes the composition of the samples.

Small Angle Neutron Scattering. All neutron scattering experiments have been performed on the instrument D11 of the Institut Max von Laue−Paul Langevin (ILL) in Grenoble (France). Due to the high flux on this instrument the data acquisition time was very short (about 3 min). The waiting time between two different shear rates was normally 10 min. We checked the steady state and approaching a shear rate either from a higher or a lower rate led to the same scattering pattern. When vesicle formation occurred, longer shearing times of up to 2 h were used. The neutron wavelength was 4.5 Å with a spread of $\Delta\lambda/\lambda = 9\%$. The static measurements were performed with 1 mm cuvettes (Hellma) covering a range of momentum transfer q from 3.5×10^{-3} to 0.44 Å^{-1}. The data were collected on a two-dimensional detector (64×64 elements of 1×1 cm^2) and corrected for background and empty cell scattering. The incoherent scattering of H_2O was used for absolute calibration according to standard procedures and software available at the ILL. Further analysis was done by radially averaging.

A Couette cell consisting of two quartz cylinders where the outer one rotated at controlled rate was used for measurements under shear. The gap was 1 mm and rectangular apertures were employed to reduce the beam size (0.25 mm × 15 mm or 1 mm × 15 mm). Two scattering configurations were used. (i) In the so-called radial position (which is the standard position) the neutron beam passes the sample along the gradient direction hence yielding information in the plane formed by flow and vorticity direction. (ii) The tangential position probes structures in the plane of gradient and vorticity direction. Here the neutron beam passes along the flow direction through the side of the Couette cell. In this configuration the path length is not uniform. Besides, there is a smearing of the directions so that the data presented with the tangential beam are only qualitative which does not, however, diminish the significance of these data. It is indeed very important to verify a correct adjustment of the beam. A feasible procedure for this adjustment consists of looking for the minimum of the transmitted intensity and to compare this minimum with the theoretical value in order to have a fixpoint.

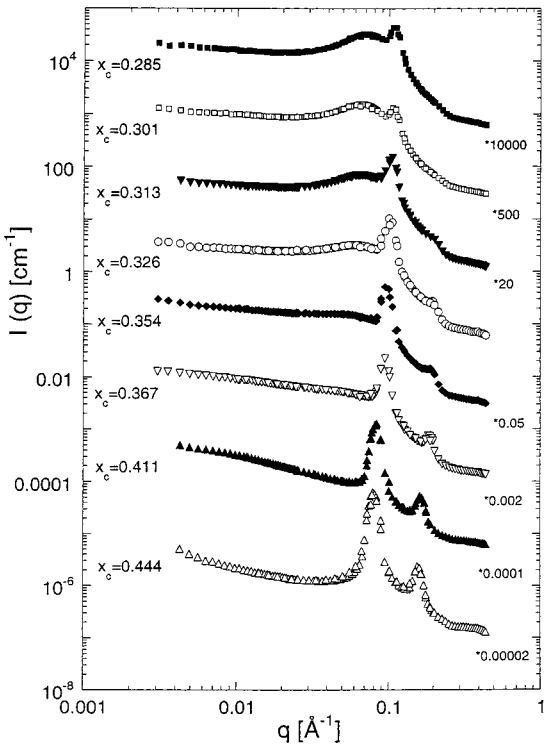

Figure 1. Absolute SANS intensity of lamellar defect phases vs momentum transfer q for samples with different decanol content.

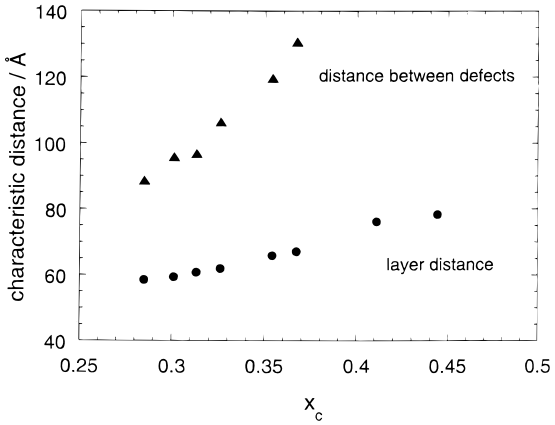

Figure 2. Lamellar spacing and mean distance between defects as a function of decanol content.

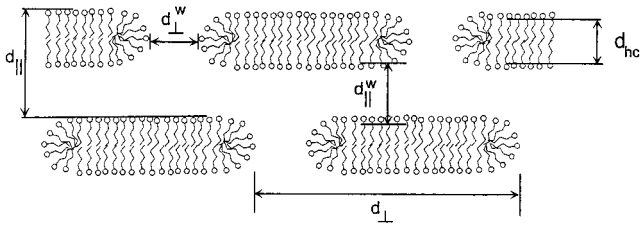

Figure 3. Parameters used for the model proposed by Holmes et al.[25]

A detailed study on the influence of the beam position will be given elsewhere. We aligned the beam in the middle of the gap using a diaphragm of 0.25 mm in order to find a good compromise concerning intensity, smearing and wall effects. We want to stress that measurements in the middle of the gap lead to asymmetric scattering patterns due to higher transmission at the outer side of the gap. Measurements near the inner side of the gap, i.e., close to the stator, cause contributions of the flow direction and could lead to misinterpretation.

For rheo-optical studies, a stress controlled Bohlin CS-10 rheometer equipped with a quartz glass 1° cone/plane shear geometry was used. For birefringence (Δn) measurements, the incident laser beam of a He−Ne laser ($\lambda_0 = 632.8$ nm) passes through the sample along the direction of the velocity gradient and perpendicular to the flow direction. The retardance was determined using the method described by Lim and Ho.[35] The actual experimental setup is given elsewhere.[36] We also used this experimental setup, slightly modified[37] for depolarized H_V small angle light-scattering (SALS) measurements under shear.

3. Experimental Results

SANS Measurements at Rest. SANS measurements on a broad q-range were performed in order to elucidate the transition from a defective to a classical lamellar phase. Figure 1 displays the scattering curves for the eight different samples. At high q one can see the Bragg reflection from the lamellar spacing. These values are in very good agreement with X-ray scattering data obtained by Berger and Hiltrop.[29] With higher decanol content the Bragg reflection became sharper and a second-order peak appeared in the q-ratio 1:2. The combination of both the decrease of the peak width and the appearance of the second-order peak indicate an increase in the positional order as the decanol content increases. This might be correlated with an increase in membrane stiffness due to increased electrostatic repulsion since the ionic surfactant is replaced by the nonionic cosurfactant decanol. For such systems it is known that the degree of dissociation of the ionic surfactant increases with increasing concentration of cosurfactant. At lower q, a broader more diffuse peak could be detected for the samples with low decanol content. This "defect peak" seems to be caused by the presence of water filled defects within the surfactant bilayer and shifted to lower q-values with higher decanol content. For the highest decanol contents the "defect peak" disappeared completely. Figure 2 shows the change in the lamellar spacing and the mean distance of these defects as a function of the SDS/decanol ratio.

We analyzed these defects according to a geometrical model proposed by Holmes and co-workers.[25] Defects present in lamellar phases could either consist of a water continuous phase (disklike micelles on planes), a surfactant continuous phase (planes pierced by holes), or a bicontinuous phase (ribbon like structure). Holmes and co-workers developed specific geometrical models for these three cases and the definition of dimension parameters is shown in Figure 3. Further details of this model are described in reference.[25] Data according to this model are listed in Table 1. Bilayer thickness d_{hc} and volume fraction were calculated according to common procedures.[28,29,38] A rather strong criterion used to distinguish between the different types of defects is the separation of the surfactants aggregates both parallel and perpendicular to the lamellae normal since for both directions the same electrostatic rules apply.[25] Therefore $d_{||}^{w}$ and $d_{\perp}^{w}$ are calculated and compared for the different models. Figure 4 displays these two distances as a function of decanol molar fraction x_c. The discoid model can be rejected because the $d_{\perp}^{w}$ values are negative for all x_c. For low decanol content x_c, a bicontinuous ribbon structure is favored since the $d_{\perp}^{w}$ values for pores are also negative. At decanol content $x_c \geq 0.34$ the defect structure changes and a surfactant continuous structures with pores is preferred. At $x_c \geq 0.4$ defects were no longer detected by SANS. This corresponds well with the change in swelling behavior found by Berger and Hiltrop indicating the transition to a defect free lamellar structure. The observed transition from a ribbonlike defect structure to pore-like

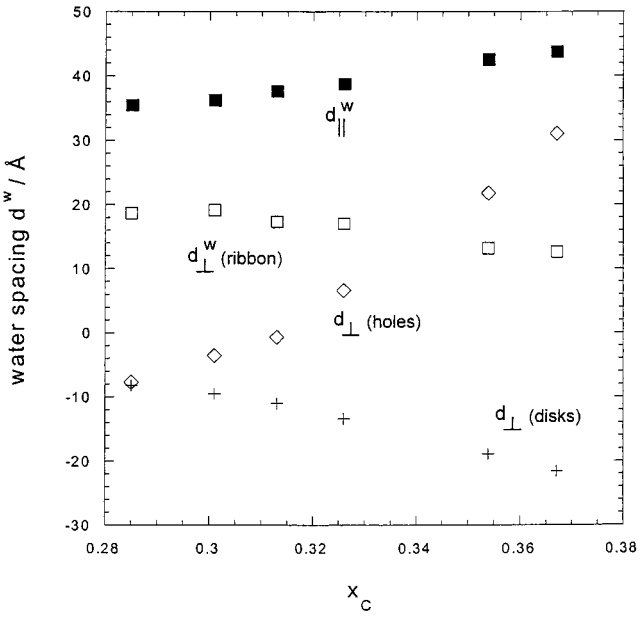

Figure 4. Water spacing plotted as function of decanol content. Closed squares, $d_{\parallel}^{w}$; open diamonds, $d_{\perp}^{w}$ (holes); open squares, $d_{\perp}^{w}$ (ribbons); crosses, $d_{\perp}^{w}$ (disks).

membrane defects and finally to a defect free lamellar phase is in good agreement with theoretical predictions.[39]

Measurements under Shear. Shear-induced structural changes were monitored for all eight different samples the compositions of which are given in Table 1. The results from four samples will be presented in more detail and finally the data of all samples will be summarized in an orientation diagram. We will focus on the following aspects. In principle, two main different processes are conceivable: (i) the orientation of the lamellae either in the parallel (*c*) or in the perpendicular (*a*) orientation or in a mixture of the two and (ii) the formation of shear induced, multilamellar vesicles. Lamellae in the transpose (*b*) orientation are disfavored and have not been observed so far in lyotropic systems.

The radial beam in SANS is crucial to detect the formation of multilamellar vesicles which lead to an isotropic Bragg scattering on the entire azimuthal trace on the two-dimensional multidetector. Thus, the enhancement of intensity along the flow direction in the Bragg peak area is a good hint to the onset of vesicle formation. Furthermore vesicles can be detected in depolarized SALS because they give rise to a characteristic four lobe scattering pattern.[12,16] The enhanced scattering also results in a reduction of the transmitted light intensity.

The tangential beam in SANS, however, is more suitable to distinguish between the parallel (*c*) and the perpendicular (*a*) orientation because lamellae with an orientation parallel to the wall of the shear cell do not contribute to the scattering in the radial beam position. We quantified the intensities of the peak maximum in all three direction of the SANS scattering patterns by averaging in 10° sectors. The intensities in the radial beam position are quantitative whereas all tangential beam data are qualitative only. To enable a comparison of the two beam positions, we shifted the intensities of the tangential beam such that the intensities in the vorticity direction (which is determined in both beam positions) match. This procedure allows to discuss orientation processes and vesicle formation in terms of intensity changes along the three principle directions: shear gradient direction, vorticity direction, and flow direction, respectively.

Sample with a low Decanol Content of $x_c = 0.301$ (Ribbon-Like Defect Structure). Figure 5 displays SANS scattering patterns from the samples with $x_c = 0.301$ for radial (left) and tangential (right) beam position at three different shear rates. Figure 6 shows peak intensities along the three directions as function of the shear rate. From these data we can distinguish three different states. Results from rheo-optics are shown in Figure 7. The existence of three different states is also obvious from viscosity, birefringence, and SALS.

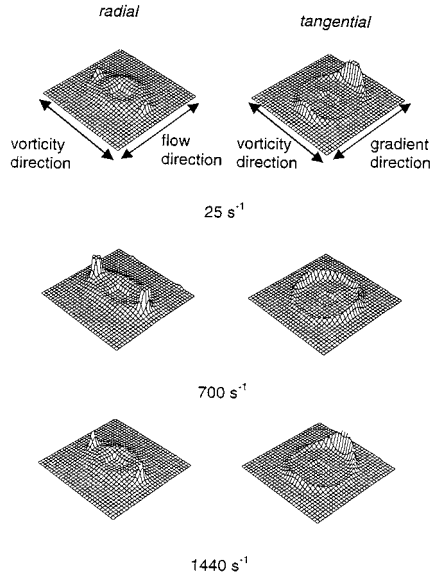

Figure 5. Neutron scattering patterns under shear of the defective lamellar phase at $x_c = 0.301$ for different shear rates of 25, 700, and 1440 s^{-1} (top to bottom). Left: radial beam. Right: tangential beam. The intensities are scaled to the same maximum for each beam direction.

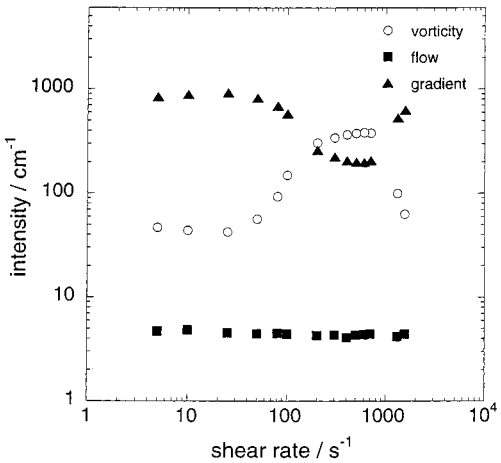

Figure 6. Shear rate dependence of averaged SANS intensities (10° sector) at $x_c = 0.301$ in gradient (triangles), vorticity (circles), and flow direction (squares). The intensities in the vorticity and the flow direction have been measured in the radial configuration (absolute intensities). The intensities in the gradient direction have been measured in the tangential beam position and shifted to allow comparison with radial data.

At low and at high shear rates, the parallel orientation is favored by a factor of approximately 10. This can be deduced from the dominating SANS intensity along the gradient direction in the tangential beam. In the radial beam position, lamellae aligned in the *c*-orientation do not contribute to the scattering. The observed Bragg peak is very weak as can be seen from a comparison with the intensity of the defect peak. The small Bragg peak is due to residual amount of lamellae still aligned perpendicularly.

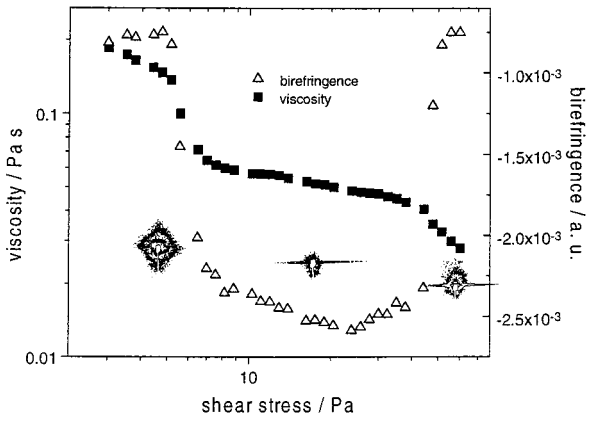

Figure 7. Viscosity, flow birefringence, and depolarized SALS pictures of the defective lamellar phase at $x_c = 0.301$ vs shear stress.

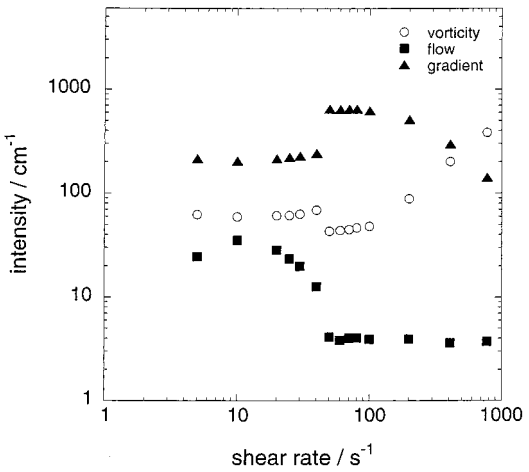

Figure 8. Averaged SANS intensities (10° sector) at $x_c = 0.313$ in gradient (triangles), vorticity (circles), and flow direction (squares).

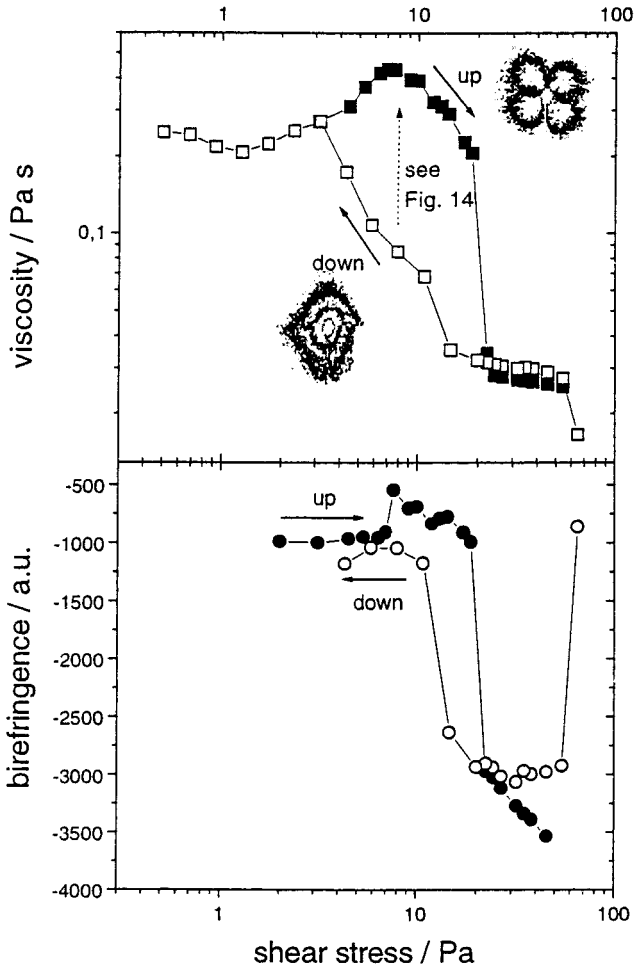

Figure 9. Viscosity and birefringence vs shear stress at $x_c = 0.313$ for measurements with increasing and decreasing shear stresses and corresponding SALS pattern for intermediate shear stresses.

At intermediate shear rates, however, the perpendicular orientation is favored (by a factor of 2). The intensity in the flow direction was very low and stayed constant over the whole range of shear rates (Figure 6). This provides clear evidence against the formation of vesicles which would lead to an enhanced Bragg scattering along the flow direction. The defect peak stayed invariant with the shear rate so that we can conclude that the defects are not affected by the shear.

The birefringence curve in Figure 7 shows low birefringence values at low and high shear rates supporting the homeotropic orientation with surfactant bilayers parallel to the walls of the shear cell. At intermediate shear rates, strong negative birefringence could be observed which indicates a perpendicular orientation of the lamellae with the long axis of the molecules aligned along the vorticity direction. The SALS-pattern clearly proof the absence of vesicles which would give rise to a four lobe pattern in H_V-scattering. At low shear rates an enhanced intensity distribution along and perpendicular to the flow direction was deteced which is in accordance with the existence of defects in the texture on a mesoscopic length scale. At intermediate shear rates a streak perpendicular to the flow direction could be observed. This indicates the presence of an ordered texture with defects along the flow direction. At very high shear rates again a streak could be observed but with less total scattering intensity with shows that less texture defects were present.

Sample with a low Decanol Content of $x_c = 0.313$ (Ribbon-Like Defect Structure). A plot of the Bragg peak intensity vs shear rate for all three directions is given in Figure 8. Compared to Figure 6 dramatic changes happened. The first transition from a parallel to a perpendicular orientation is shifted to higher shear rates (500 s^{-1} as compared to 100 s^{-1}) and the second reorientation could not be observed at shear rates accessible with SANS. At low shear rates (20−60 s^{-1}) the formation of multilamellar vesicles could be observed. This can clearly be seen from the intensity in flow direction. It remained constant for all shear rates in Figure 6 ($x_c = 0.301$). For $x_c = 0.313$, the intensity along the flow direction was higher, due to the presence of vesicles, see Figure 8. The point, when the vesicles were destroyed can be seen in the abrupt change of scattering intensities: the intensity in flow direction sharply decreased (and then remained constant at higher rates) and slightly decreased along the vorticity direction, while the intensity in the gradient direction increased.

Results from rheo-optics are shown in Figure 9. In this figure we distinguish between data which have been obtained while increasing the stress ("up") on one hand and data with decreasing shear stress ("down") on the other hand. While similar behavior was observed at low and high shear stresses, different behavior was found at intermediate stresses. Increasing the shear stress led to a vesicle formation which can be deduced already from the increase of viscosity. The shear induced formation of multilamellar vesicles is confirmed by the detection of the four lobe scattering pattern in depolarized SALS. Higher stresses reduced the size of the vesicles and finally destroyed them above

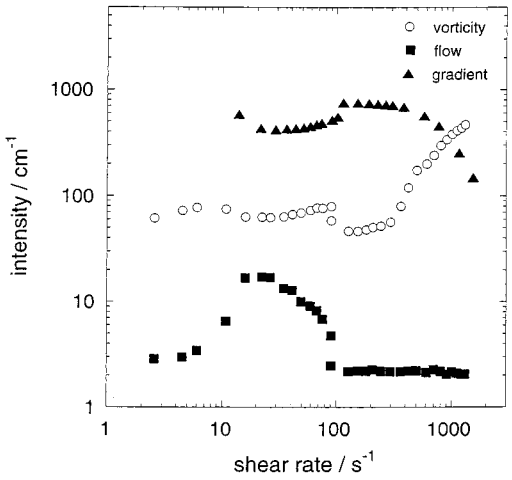

Figure 10. Averaged SANS intensities (10° sector) at $x_c = 0.354$ in gradient (triangles), vorticity (circles), and flow direction (squares).

a critical stress of ca. 20Pa and then the system changed to the perpendicular orientation of lamellae. In the perpendicular orientation the viscosity remained at a constant plateau until the second reentrant transition to the parallel orientation lowered the viscosity again.

Different behavior was found with the "down curve". Reducing the shear stress after having presheared the sample in the perpendicular orientation led to a state with a lower viscosity as compared to the "up curve" in a stress range from 20 to 4 Pa. A different scattering pattern typical of texture defects was observed in depolarized SALS, and the four-lobe pattern was only observed at low stresses. Obviously, vesicles have not been formed at intermediate stresses during the "down-curve" but only at stresses below 4 Pa.

The birefringence curves in Figure 9, however, are similar for the up and down experiments and the transition to/from strongly negative Δn-values was found in both cases. The absolute birefringence value is small for both vesicles and parallel aligned lamellae and therefore this technique is not suitable to distinguish between these two states.

With SALS, however, a distinction is possible. The four-lobe scattering pattern typical for the "up curve" clearly corresponds to multilamellar vesicles while the state which can be reached by decreasing the stress can be characterized as a parallel orientation *c*. Furthermore, the turbidity of the multilamellar vesicle state is much higher than for lamellae in the parallel orientation. Thus in the "up curve" a transition from MLVs to the perpendicular orientation was observed at intermediate stresses whereas a transition from perpendicular to parallel orientation and then to vesicles was found with the "down curve". The question which state corresponds to the steady state will be discussed below.

The SANS data in Figure 8 revealed an increase of intensity along the gradient direction at shear rates above 40 s^{-1} when the vesicles were degraded. This also indicates the existence of parallel aligned lamellae between the vesicle state and the perpendicular orientation, respectively. Identical SANS spectra were detected for up and down measurements but one has to keep in mind that the SANS experiments have been performed at controlled shear rate whereas a controlled shear stress was applied in the rheo-optical experiments. Differences between stress and rate controlled experiments will be discussed below.

Sample with an Intermediate Decanol Content of $x_c = 0.354$ (Porelike Defect Structure). Figure 10 displays the dependence of SANS peak intensities on shear rate for a sample exhibiting

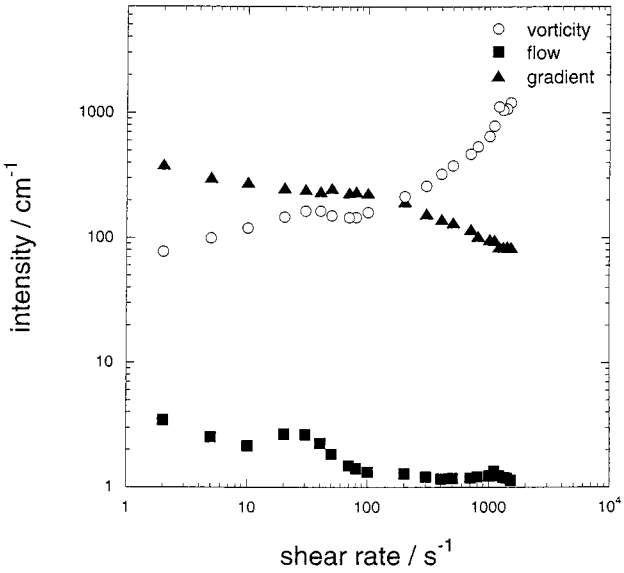

Figure 11. Averaged SANS intensities (10° sector) at $x_c = 0.411$ in gradient (triangles), vorticity (circles), and flow direction (squares).

a pore like defect structure with a decanol content of $x_c = 0.354$. Although the defect structure is different from the sample with $x_c = 0.326$, the shear rate dependent behavior is quite similar. At high shear rates a reorientation from *c* to *a* takes place. The formation of the multilamellar vesicles, characterized by the same abrupt changes in intensities, now starts at shear rates of about 10 s^{-1}. At very low shear rates ($\sim$5 s^{-1}), however, the vesicles are destroyed and the lamellae orient parallel to the wall again (*c*-orientation). To prove the vesicle formation we performed SALS measurements and turbidity measurements. Under shear the vesicles are elongated. This can be seen from the enhanced SANS intensity in the vorticity direction of as compared to the flow direction. In addition to this, lamellae may be still present in the vesicular system.

Sample with High Decanol Content of $x_c = 0.411$ (Defect Free Lamellar Phase). The peak intensities in the three different directions for a sample without defects is shown in Figure 11. The most striking difference compared to the last two samples is the lack of vesicle formation. The intensity in the flow direction stayed on a very low level (compare with Figure 10). The intensities in gradient and vorticity direction are much higher and display no abrupt changes. At high shear rates also a reorientation from *c*- to *a*-orientation could be observed, whereas the *c*-orientation is stable up to very low shear rates.

4. Discussion

The samples investigated in this study exhibited two general features: (i) reorientation of lamellae and (ii) shear-induced vesicle formation. One can clearly distinguish between the parallel and the perpendicular orientation by means of SANS obtained with radial and tangential beam as well as with birefringence. The vesicle formation can be easily detected by an increase of viscosity, depolarized SALS, and turbidity measurements. For both kinds of transitions, however, there might be a difference whether the shear stress or the shear rate is controlled. There has been much discussion about this topic in recent work.[12,40,41] To unambiguously clarify this problem all measurements have to be performed under both constant rate and constant stress control which, however, is not possible at the moment with our equipment for SANS. Nevertheless, we want to focus on some aspects that may clarify relevant parts in this discussion. A second point one has to pay attention to is

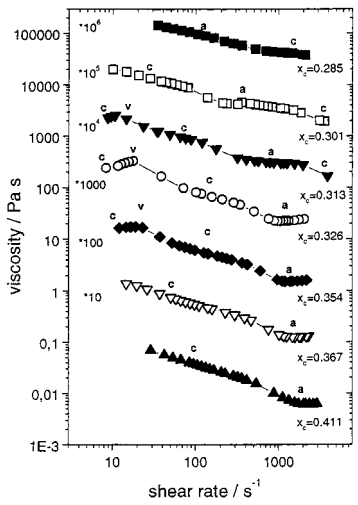

Figure 12. Viscosity vs shear rate for all samples ("down curve").

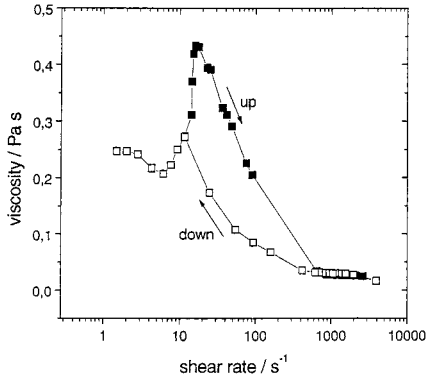

Figure 13. Viscosity vs shear rate for $x_c = 0.313$ for "up" and "down" measurement.

the possibility that the kinetics of the various transitions can be rather slow. It turned out that the time dependence is more crucial when vesicles are involved. Vesicle formation can be extremely slow depending on sample and shear history. Therefore we performed some long-time measurements (waiting time for steady state up to 6 h).

Rheo-optical experiments were performed under controlled stress conditions. At high shear stresses the viscosity curves showed a plateau for all samples when the *a*-orientation was reached. With increasing decanol content a decrease of the plateau value was found. Figure 12 shows the viscosity curves for all samples. The measurements in this series have been performed with *decreasing* shear stresses in order to avoid the influence of the sample history. For sake of comparability with the SANS data, we plotted the viscosity vs shear rate. Lowering the stress generally led to a transition from the *a*-orientation to the *c*-orientation which was accompanied by a kink in the flow curve. The formation of vesicles for the sample with intermediate decanol content can be seen from the viscosity maximum which, however, was not so pronounced as with "up curves". We therefore characterized the behavior of the sample with $x_c = 0.313$ in detail.

In Figure 13 results from both types of experiments are displayed now plotted vs shear-rate. The experiment starting with low shear stresses ("up") led to an immediate vesicle formation at low stresses and was characterized by a pronounced increase in viscosity. Further increase of the shear stress, however, did not create a parallel orientation as in the measurement with decreasing shear stresses. Once a critical shear stress was reached, the viscosity curve exhibited a jump in the shear

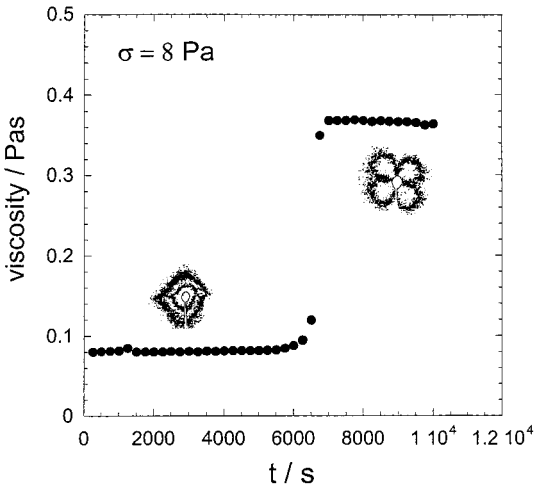

Figure 14. Time dependent measurement for $x_c = 0.313$ at a constant shear stress of 8 Pa. Viscosity and depolarized SALS pictures.

rate leading directly to the plateau of the *a*-orientation. In this region where the jump in shear rate was found, a parallel orientation can be detected when lowering the shear stresses ("down"). To check for steady states, we performed long term measurements with constant shear stress in a region where either vesicles were present in the "up curve" or lamellae with a parallel orientation were present in the "down curve", see Figure 14. We started at a stress of 8 Pa with a sample, which has been in the perpendicular orientation before (see Figure 9). Soon a viscosity plateau was reached which was stable for approximately 2 h. After this time, suddenly a transition from the parallel orientation to a vesicle state took place within ca. 15 min. Finally a second plateau was reached which can be characterized as a vesicular state as can be seen by the change in the light scattering pattern. Obviously, the parallel orientation was only a metastable state at this shear stress.

The situation becomes even more complicated when constant shear rate experiments are considered. As mentioned above, the vesicle were degraded above a certain critical shear stress leading to a jump in the shear rate. When, however, the vesicle solution was subjected to a constant intermediate shear rate (e.g., 200 s^{-1}), a mixed state was then obtained. Apparently, a constant stress is necessary to completely transform vesicles to aligned lamellae. In other words, an energetic barrier has to be crossed. Similar results have been obtained in other systems.[42,43] but more experiments are necessary to completely understand the vesicle degradation.

The kinetics of the vesicle formation seem to be dependent on both shear history and the stress applied. The higher the stresses are the longer it took until the vesicle formation started. We repeated this measurement a couple of times and always found this transition with shearing times between 2 and 5 h. However, it was not possible correlate the onset of vesicle formation with shear time or strain. This is different to results reported by Bergenholtz and Wagner who could superpose different curves when plotted vs the total deformation.[12] They, however, investigated the vesicle formation starting at low stresses, whereas the data in Figure 14 correspond to a sample presheared at high stresses.

From this observation we speculate that the vesicle formation is correlated with the concentration and orientation of texture defects as, e.g., screw dislocations. At low stresses, lots of texture defects were present and the vesicle formation started immediately. Texture defects are visible in optical microscopy and also give rise to a high light scattering intensity. At high

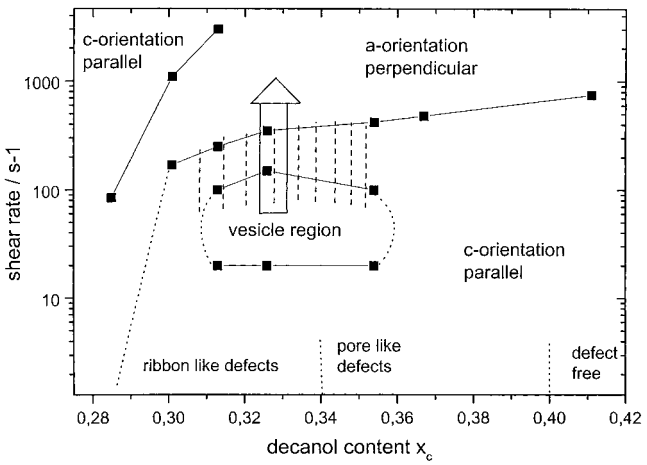

Figure 15. Orientation diagram of the system SDS/decanol/water as function of the decanol content (see text).

shear stresses, a less intense streak was observed in SALS indicating that less defects were present which were aligned along the flow direction. Apparently, the concentration of defects was low when the sample was presheared at high stress and this increased the nucleation time for vesicle formation when the stress was reduced. The reduction of shear stress first led to a reorientation of lamellae and the SALS pattern changed indicating the formation of texture defects. Once the initial nucleation occurred, vesicle formation was completed within about 20 min. It seems as if lamellae in the parallel orientation must be present in order to obtain vesicle formation. We never observed vesicle formation at shear stresses, which are in the range where the perpendicular orientation dominates.

The different regions of shear induced states are summarized in terms of an orientation diagram where we display the different shear regions as a function of the decanol content in the surfactant/cosurfactant mixture, see Figure 15. First we wish to discuss the different features of the orientation diagram before comparing our data with other work on surfactants and block copolymers. The parallel orientation *c* of the lamellae is the preferred one at low shear rates for all samples except for the sample with the lowest decanol content. At the lowest decanol content, the perpendicular orientation *a* was found down to very low shear rates but it cannot be excluded that the *c* reorientation could eventually occur but this is difficult to detect because of the long times needed to reach steady state. For higher shear rates either shear induced vesicle formation or reorientations have been observed. The samples with the lowest decanol content (the highest defect concentration in the membrane) showed no vesicle formation within the time scale studied here (up to 10 h). In the intermediate shear rate regime the perpendicular orientation *a* was preferred. For very high shear rates the samples with very low decanol content revealed a second reorientation to the parallel orientation *c*. Vesicle formation was observed for decanol contents between $0.31 < x_c < 0.35$. For higher or lower decanol content we found no indication for vesicle formation within shearing times of several hours. As Figure 14 shows this does not exclude the vesicle state explicitly because vesicle formation could last rather long. So the border at minimum and maximum decanol content (i.e., in the horizontal direction in Figure 15) necessary for vesicle formation are valid for shearing times of up to a maximum of 10 h.

The end of the vesicle regime in the vertical direction is difficult to determine because a two-phase region is entered by using constant rate as SANS experiments revealed. This can be seen at the intensity in the flow direction which is changing continuously until it reaches the plateau value. Measurements under constant stress directly lead to a jump to the *a*-orientation as indicated with the broad arrow in the orientation diagram.

The orientation diagram presented in Figure 15 is not in contradiction with work done by other groups but more like an extension to former investigations. The first studies of Diat et al. revealed three states of orientation, a parallel at both low and high shear rates and a vesicle state at intermediate shear rates. This behavior is similar for the samples in this study up to high, but not to very high shear rates, and only when the applied shear rate is controlled. In addition to this, we observe a reorientation to the perpendicular lamellae orientation at higher shear rates. This reorientation has also been observed by Mang et al. and by Penfold et al. These groups, however, have not observed both reorientation and vesicle formation in one sample. This case is also included in our orientation diagram for high decanol content. The mixed state of parallel and perpendicular orientation found by Penfold and co-workers and also by us with SANS can only be found by using constant rate control. Constant stress measurements providing enough waiting time to reach the steady-state always lead to a jump from the parallel to the perpendicular orientation. This observation is quite general for all kinds of transitions we described so far.

The behavior of block copolymer melts which are mostly investigated under oscillatory shear revealed a reorientation from parallel to a perpendicular alignment at intermediate amplitudes and a reentrant transition to parallel alignment at high amplitudes and frequencies.[5] So far, vesicles have not been found in block copolymer melts. A comparable behavior exhibiting also the re-entrant transition to parallel is also included in our orientation diagram for samples with low decanol content. From this we guess that the orientation processes are a general feature of lamellar phases while the vesicle formation seems to be restricted to lyotropic systems so far. This might be due to special texture defects rather than to molecular properties of the membrane.

There have been many models and speculations to explain both the reorientation and the vesicle formation. While the processes responsible for the reorientation seem to be at least partly understood, the vesicle formation still remains unclear. From our investigation we can conclude that membrane defects are not directly correlated with the vesicle formation under shear because samples with different membrane defects show similar behavior in rheology. Vesicle formation seems to start only from the parallel orientation with different time scales necessary for nucleation at different shear stresses. We speculate that texture defects are responsible for the differences in the onset of the vesicle formation and that the vesicular state is a state of the lamellar phase with a well-defined concentration and distribution of defects in the texture. More work needs to be done to conclude and compare orientation diagrams with both the shear rate and the shear stress as parameter.

5. Conclusion

The influence of shear on lamellar phases of the system SDS/decanol/water with different membrane defects was studied. As described by a theoretical investigation[39] we found transitions from a bicontinuous structure of ribbon like defects to a surfactant continuous structure with pore like defects and finally to a defect free classical lamellar phase. In addition to former investigations[24] we could distinguish between those different kinds of membrane defects.

The influence of shear on the lamellar phase with different membrane defect structure is summarized in the orientation

diagram in Figure 15. As general behavior, all samples showed a reorientation of the lamellae. Some samples with low decanol content even show a reentrant orientation to parallel alignment at very high shear rates, a feature which has only been observed for block-copolymer systems so far. The formation of vesicles has been found in a broad range of surfactant-cosurfactant ratio embedded in the region of parallel orientation. Neither the defective structure of the membrane nor the reentrant orientation seems to be directly linked with the vesicle formation. Vesicle formation seems to depend on textural defects.

Apparently, the orientation processes are a general feature of samples with lamellar morphology while the vesicle formation seems to be restricted to lyotropic systems.

Acknowledgment. We thank the Deutsche Forschungsgemeinschaft for financial support. J. Z. gratefully acknowledges a Marie-Curie research fellowship of the European Commission.

References and Notes

(1) Herb, C. A., Prudi'homme, R. K., Eds. *Structure and Flow in Surfactant Solution*; ACS Symposium Series 578; American Chemical Society: Washington, DC, 1994.

(2) Nakatani, A. I., Dadmun, M. D., Eds. *Flow-Induced Structures in Polymers*; ACS Symposium Series 597; American Chemical Society: Washington, DC, 1995.

(3) Mortensen, K. *J. Phys. Condens. Matter* **1996**, *8*, A103.

(4) C. R. Safinya, C. R.; Sirota, E. B.; Bruinsma, R. F.; Jeppesen, C.; Plano, R.; Wenzel, L. *Science* **1993**, *261*, 588.

(5) Maring, D.; Wiesner, U. *Macromolecules* **1997**, *30*, 660.

(6) Chen, Z.-R.; Kornfield, J. A.; Smith, S. D.; Grothaus, J. T.; Satkowski, M. M. *Science* **1997**, *277*, 1248.

(7) Fredrickson, G. H.; Bates, F. S. *Annu. Rev. Mater. Sci.* **1996**, *26*, 501.

(8) Cates, M.; Milner, S. F. *Phys. Rev. Lett.* **1989**, *62*, 1865.

(9) Fredrickson, G. H. *J. Rheol.* **1994**, *28*, 1045.

(10) Diat, O.; Nallet, F.; Roux, D. *J. Phys. II* **1993**, *3*, 1427.

(11) Mang, J. T.; Kumar, S.; Hammouda, B. *Europhys. Lett.* **1994**, *28*, 489.

(12) Bergenholtz, J.; Wagner, N. *Langmuir* **1996**, *12*, 3122.

(13) Penfold, J.; Staples, E.; Khan Lodhi, A.; Tucker, I.; Tiddy, G. J. T. *J. Phys. Chem. B* **1997**, *101*, 66.

(14) Olsson, U.; Mortensen, K. *J. Phys. II* **1995**, *5*, 789.

(15) Penfold, J.; Staples, E.; Tucker, I.; Tiddy, G. J. T.; Kahn Lodhi, A. *J. Appl. Crystallogr.* **1997**, *30*, 744.

(16) Weigel, R.; Läuger, J.; Richtering, W.; Lindner, P. *J. Phys. II* **1996**, *6*, 529.

(17) Lukaschek, M.; Müller, S.; Hasenhindl, A.; Grabowski, D. A.; Schmidt, C. *Colloid Polym. Sci.* **1996**, *274*, 1.

(18) Zipfel, J.; Lindner, P.; Tsianou, M.; Alexandridis, P.; Richtering, W. *Langmuir* **1999**, *15*. In press.

(19) Diat, O.; Roux, D.; Nallet, F. *Phys. Rev. E.* **1995**, *51*, 3296.

(20) Sierro, P.; Roux, D. *Phys. Rev. Lett.* **1997**, *78*, 1496.

(21) Bergmeier, M.; Hoffmann, H.; Thunig, C. *J. Phys. Chem. B* **1997**, *101*, 5767.

(22) Bergmeier, M.; Gradzielski, M.; Hoffmann, H.; Mortensen, K. *J. Phys. Chem. B* **1998**, *102*, 2837.

(23) Zipfel, J.; Lindner, P.; Richtering, W. *Phys. B* **1998**, *241*−*243*, 1002.

(24) Leaver, M. S.; Holmes, M. C. *J. Phys. II* **1993**, *3*, 105.

(25) Holmes, M. C.; Smith, A. M.; Leaver, M. S. *J. Phys. II* **1993**, 1357.

(26) Holmes, M. C.; Leaver, M. S.; Smith, A. M. *Langmuir* **1995**, *11*, 356.

(27) Hendrikx, Y.; Charvolin, J. *Liq. Cryst.* **1987**, *3*, 265.

(28) Quist, P. O.; Halle, B. *Phys. Rev. E* **1993**, *47*, 3374.

(29) Berger, K.; Hiltrop, K. *Colloid Polym. Sci.* **1996**, *274*, 269.

(30) Berghausen, J.; Zipfel, J., Lindner, P.; Richtering, W. *Europhys. Lett.* **1998**, *43*, 683.

(31) Mahjoub, H. F.; Bourgaux, C.; Sergot, P.; Kleman, M. *Phys. Rev. Lett.* **1998**, *81*, 2076.

(32) Zipfel, J.; Lindner, P.; Richtering, W. *Prog. Colloid Polym. Sci.* **1998**, *110*, 139.

(33) Läuger, J.; Weigel, R.; Berger, K.; Hiltrop, K.; Richtering, W. *J. Colloid Interface Sci.* **1996**, *181*, 521.

(34) Gustafsson, J.; Orädd, G.; Nyden, M.; Hansson, P.; Almgren, M. *Langmuir* **1998**, *14*, 4987.

(35) Lim, K.-C.; Ho, J. T. *Mol. Cryst. Liq. Cryst.* **1978**, *47*, 225.

(36) Schmidt, J.; Weigel, R.; Burchard, W.; Richtering, W. *Macromol. Symp.* **1997**, *120*, 247.

(37) Berghausen, J.; Fuchs, J.; Richtering, W. *Macromolecules* **1997**, *30*, 7574.

(38) Tanford, C. *The Hydrophobic Effect*, 2nd ed.; Wiley: New York, 1980.

(39) Bagdassarian, C. K.; Roux, D.; Avinoam, B. S.; Gelbart, W. J. *Chem. Phys.* **1991**, *94*, 3030.

(40) van der Linden, E.; Hogervorst, W. T.; Lekkerkerker, H. N. W. *Langmuir* **1996**, *12*, 3127.

(41) Panizza, P.; Colin, A.; Coulon, D.; Roux, D. *Eur. Phys. J. B* **1998**, *4*, 65−74.

(42) Bonn, D.; Meunier, J.; Greffier, O.; Al-Kahwaji, A.; Kellay, H. *Phys. Rev. E.* **1998**, *58*, 2115.

(43) Schmidt, G. Ph.D. Thesis, Freiburg, 1998, manuscript in preparation.